Maria V. Piaggio[1]
Marta B. Peirotti[2]
Julio A. Deiber[2]

[1]Cátedra de Bioquímica Básica de Macromoléculas, Facultad de Bioquímica y Ciencias Biológicas, Universidad Nacional del Litoral (UNL), Santa Fe, Argentina
[2]Instituto de Desarrollo Tecnológico para la Industria Química (INTEC), UNL, Consejo Nacional de Investigaciones Científicas y Técnicas (CONICET), Santa Fe, Argentina

Received February 24, 2010
Revised March 31, 2010
Accepted April 1, 2010

Research Article

Estimation of global structural and transport properties of peptides through the modeling of their CZE mobility data

Peptide electrophoretic mobility data are interpreted through a physicochemical CZE model, providing estimates of the equivalent hydrodynamic radius, hydration, effective and total charge numbers, actual ionizing p*K*, pH-near molecule and electrical permittivity of peptide domain, among other basic properties. In this study, they are used to estimate some peptide global structural properties proposed, providing thus a distinction among different peptides. Therefore, the solvent drag on the peptide is obtained through a characteristic friction power coefficient of the number of amino acid residues, defined from the global chain conformation in solution. As modeling of the effective electrophoretic mobility of peptides is carried out in terms of particle hydrodynamic size and shape coupled to hydration and effective charge, a packing dimension related to chain conformation within the peptide domain may be defined. In addition, the effective and total charge number fractions of peptides provide some clues on the interpretation of chain conformations within the framework of scaling laws. Furthermore, the model estimates transport properties, such as sedimentation, friction and diffusion coefficients. As the relative numbers of ionizing, polar and non-polar amino acid residues vary in peptides, their global structural properties defined here change appreciably. Needs for further research are also discussed.

Keywords: Electrical charge fractions / Friction power coefficient / Packing dimension / Peptide diffusion coefficient / Peptide electrophoretic mobility
DOI 10.1002/jssc.201000134

1 Introduction

CZE is a successful analytical technique devoted to the separation of both electrically charged macromolecules and small ionic species. In this framework, peptides have been intensively studied together with the proposal of optimal running protocols and new experimental setups (see [1–4] and citations therein). Interesting is the fact that different types of models to interpret effective electrophoretic mobility data may provide additional physicochemical properties and structural characterization of these analytes [5–15]. Thus, the problem in general is formulated as follows: given basic running protocols with well-specified solvent bulk pH, ionic strength I, temperature T, electrical permittivity ε and viscosity η, together with peptide molar mass M and amino acid sequence (AAS) of N amino acid residues, a model based on well-established physicochemical theories and true properties is desired to characterize peptides separated in CZE runs. The model target is to fit or predict the effective electrophoretic mobility data of these analytes, resulting in numerical values of basic physicochemical properties. Then, they are used to infer global structural properties associated with the physics of peptide chains in dilute solution. In this framework, there are CZE models for peptides and proteins in the literature, covering different aspects and phenomena with varied degrees of complexity [5, 8–11, 13–20]. By considering these works on the subject concerning either asymptotic analytical solutions and complex computational works, here we propose to add some theoretical developments to our previous studies [10, 13], involving the simple Perturbed Linderstrøm–Lang capillary electrophoresis model (PLLCEM), which has been applied previously to amino acids, peptides and proteins. The description and development of this model may be found in detail with appropriate hypothesis and limitations in [18–20]. In particular, this model allowed us to carry out studies of peptide characterizations through the ''inverse problem'' [10, 13], where the effective mobility was provided as one of the input data and then some basic peptide physicochemical properties were predicted.

At present, it has been recognized in the literature [21–24] the need to provide global structural properties of peptides and proteins apart from their local structural data usually obtained through NMR, circular dichroism and

Correspondence: Dr. Julio A. Deiber, INTEC, Güemes 3450, S3000GLN, Santa Fe, Argentina
E-mail: treoflu@santafe-conicet.gob.ar
Fax: +54-342-4550944

Abbreviations: AAS, amino acid sequence; **PLLCEM,** perturbed Linderstrøm–Lang capillary electrophoresis model

X-ray crystallography in conjunction with the AAS. While these techniques determine the occurrence of specific secondary structural motifs, such as α-helixes, β-strands, reversed turns, random coils, *etc.*, one also expects to obtain global shape descriptors as well as the estimation of useful transport properties of these biomacromolecules. Therefore, in relation to details of biological relevance, it is expected that the definitions of global structural properties of peptides must be sensitive to their microstructure, involving the complex distribution of possible secondary conformations, which in turn are a result of both the AAS and the solvent type, where these chains are immersed [25–27]. It is also important to visualize here that peptides in solution are electrically charged hetero-chains (N amino acid residues randomly distributed in a chain building up a biopolyampholyte), where one finds an interplay among different side groups involving hydrophobic, dispersion and electrostatic forces, within a hydrated microenvironment of weak-bonded water molecules. It is then clear that these macromolecules present additional conformational complexities in relation to those found in synthetic uncharged and polyampholytic homo-chains and block-chains, for which global structural properties are better established (see, for instance, [28–31] and citations therein).

Therefore, within the prediction capability of the PLLCEM, the present study is concerned with the estimation of some global structural properties of peptides defined and derived here from the basic physicochemical properties provided by this model. These structural properties, defined below in Section 2, are associated with the peptide electrical state, such as the effective charge $\Delta\sigma$ and total charge σ number fractions [29, 31]. Other global structural properties resulting from peptide average chain conformations and hydrations are the packing dimension g_p of the chain within its hydrodynamic volume V_H, and the friction power coefficient g_f, to which N is raised to obtain the average solvent drag on the chain (peptide friction), both defined in Section 2.

Therefore, the present study is organized as follows. Section 2 describes briefly the main PLLCEM numerical outputs, which allow then a presentation of global structural properties defined here. Section 3 discusses this type of peptide characterization with specific case studies. In addition, estimations of peptide transport properties, such as average sedimentation s, friction f and diffusion D coefficients are provided. For this purpose, a set of 102 peptides studied *via* CZE at pH 2.5, $T = 22^{\circ}C$ and $I = 35.6$ mM, and reported previously in the literature [32, 33] was selected here. Needs for further research are also proposed to deepen the development of global structural properties of peptides.

2 Global structural and transport properties of peptides

From the PLLCEM relevant basic peptide properties may be evaluated [13, 20], such as positive Z_+, negative Z_-, effective $Z = |Z_+| - |Z_-|$ and total $Z_T = |Z_+| + |Z_-|$ charge numbers, and Stokes or equivalent hydrodynamic radius a_H, defining the total hydrodynamic peptide volume $V_H = 4\pi a_H^3/3$. This volume is decomposed into the peptide compact volume $V_c = Mv_p/N_A = 4\pi a_c^3/3$ with compact radius a_c and the hydration volume V_w. Here, N_A is the Avogadro constant, M the peptide molar mass and v_p the average peptide-specific volume calculated through $v_p = \sum_{i=1}^{N} (M_i v_i/M)$[13], where v_i is the specific volume and M_i the molar mass of each amino acid residue composing the AAS. As $a_H > a_c$ due to the water associated with the peptide [10, 13], an estimate of hydration δ (water mass/peptide mass) is obtained from $\delta \approx [(a_H/a_c)^3 - 1](v_p/v_w)$[13]. Here, v_w is the specific volume of the protocol solvent. In addition, estimations of peptide hydration number $H = \delta M/18$ (number of water molecules *per* peptide chain) are obtained by summing each hydration number of ionizing, polar and non-polar groups [13, 19] (these last expressions establish the PLLCEM convergence criterion [19, 20]). In addition, this model provides the pK_i values of ionizing groups yielding a shift ΔpK_i in the reference pK_i^r reported in [34] as a result of the charge regulation phenomenon present in these particles [18, 35]. Therefore, the pH microenvironment pH_i around the i-ionizing group is also numerically available [19]. This pH_i is a function of the mean field pH^*, designated the near-molecule pH, and the electrical permittivity within the peptide domain ε' (see the numerical procedure in [20] for their estimations). In this framework, the frequent assumption $\varepsilon' \approx \varepsilon$ is substituted by the expression $\varepsilon' = \varepsilon\delta/(1+\delta) + \varepsilon_p/(1+\delta)$, which uses the particle hydration as the weighing parameter between peptide ε_p [36] and solvent ε electrical permittivities.

Therefore, to apply the PLLCEM to a peptide by inputting its effective mobility μ_p, the other relevant equation is $\mu_p = \Omega\mu$ [13], where $\mu = eZf(\kappa a_H)/6\pi\eta a_H(1+\kappa a_H)$ is the effective mobility of the equivalent spherical problem, $f(\kappa a_H)$ Henry's function, $\kappa = \sqrt{2e^2 N_A I 10^3/\varepsilon k_B T}$ the inverse of the screening length and k_B the Boltzmann constant. In the expression for μ_p, the shape-orientation factor $\Omega = 6\pi\eta a_H/f$[10] associated with the particle shape and orientation density distribution function may be further modeled, for instance, through equations providing the effective mobility of cylindrical or spheroidal particles [10, 13, 20]. In this particular aspect, the peptide friction in the electrophoretic movement is modeled through a particle that preserves the hydrodynamic volume $V_H = V_c + V_w$ having also the right f achieved through the characteristic particle shape. This specific point was first described and discussed in [37] with some detail for globular proteins *via* empirical estimations of δ, and at present relevant works have also emerged, with particular emphasis to describe computationally the closer surface shape that relates to the actual furry protein shape in solution as inferred from NMR and X-ray crystallographic experiments [16, 38, 39]. For the particular case of peptides, an interesting proposal is the bead chain model [11, 14], where the sizes of amino acid residues are considered. Within the PLLCEM framework,

the basic characterization of peptides and proteins is obtained, as a first approximation, directly with parameters Ω and a_H [13, 20] and the charge state defined through Z and Z_T, allowing then the application of an appropriate chain or particle model that is compatible with the average value of the peptide friction (the average orientation of the main particle axis is included in Ω [13]). It is then clear that in the context of the ''equivalent spherical model'' [10, 13, 20], several hydrodynamic particles may be adopted and determined through parameters a_H and Ω. Although in the previous works [10, 13, 20], the PLLCEM considered cylindrical and spheroidal particle shapes, here we also express the peptide friction through the friction power coefficient defined below. Furthermore, despite the numerical procedure used in the PLLCEM has been provided and discussed in [10, 13, 18–20] for both peptides and proteins, in the present Supporting Information, freely available through the link provided by the journal, one may find a list of all symbols used here and a summary of the main steps involved in the numerical procedure of this model.

From the above framework, several peptide global structural properties may be introduced now. The analysis of peptide packing within the hydrodynamic volume defined through a_H requires the consideration of the average monomer radius $a_o = \sum_{i=1}^{N} a_i/N$ [20] (different monomers forming the hetero-chain are considered), where each amino acid residue has a radius $a_i = \{3\nu_i M_i/(4\pi N_A)\}^3$. Therefore, by observing that one unit of equivalent hydrodynamic radius a_H is equal to N units of amino acid residues with average radius a_o, the chain packing dimension g_p may be expressed as [20, 40],

$$g_p = \log N/\log(a_H/a_o) \leq 3 \quad (1)$$

For $g_p = 3$ the peptide compact volume results, with $a_H = a_c$ and $\delta = 0$. Thus, in general, values of a_H and g_p carry in some degree condensed peptide structural information for further analysis.

The average peptide friction is $f = 6\pi\eta a_o N^{g_f}$, indicating that $g_f \leq 1$ [28, 41]. Thus, the maximum peptide friction is achieved for $g_f = 1$, when a free draining chain in creeping flow with negligible intra-chain hydrodynamic interaction is considered [28]. Furthermore, when hydrodynamic interaction among chain units is present $1/3 < g_f < 1$ for both electrically neutral and charged chains [30, 31]. These limit values for either the neutral homo-chains and the polyampholyte hetero-chains (peptides) are obtained through different mechanisms. In the former chains, they relate mainly to the effect of solvent quality and temperature, while in the later ones, they are due significantly to the electrical state of particles for a given solvent and temperature [29–31].

Therefore, from the expressions for Ω and f, one readily shows that

$$g_f = \frac{1}{g_p} - \frac{\log\Omega}{\log N} \quad (2)$$

Equation (2) indicates that for spherical particles, and to a good approximation for aspherical particles with a random flight orientation distribution function of their major axes ($\Omega \approx 1$) [13, 20], the power friction coefficient satisfies $g_f = 1/g_p$, which are particular cases and the less frequent ones, as shown below. In addition, for ideal chains $g_f \approx 1/2$, while for globular polyampholytes when fluctuation-attractive electrostatic interactions are relevant (or when the solvent is poor for neutral chains) $g_f \approx 1/3$ [30, 31, 42], yielding a collapsed globule conformation. For self-avoiding random polyampholytes, $g_f \approx 3/5$ (see below).

Additional global structural properties considered here are those associated with the peptide electrical state, such as the effective $\Delta\sigma = |Z|/N$ and the total $\sigma = Z_T/N$ charge number fractions. The importance of these global properties is that for chains in dilute solution free of salt, they satisfy simple scaling relationships [29, 31], suggesting four possible global chain conformational states for polyampholytes in general (peptides in this study). As the PLLCEM provides g_f, here we modify these scaling relationships by introducing the chain gyration radius $R \approx a_o N^{g_f}$ into the Debye radius due to charges, expressed as $r_D \approx (R^3/l_B N\sigma)^{1/2}$, and defined in [29, 43]. Therefore, the following ranges of coordinates $\Delta\sigma$ and σ delimiting different chain conformational states are obtained: (i) $\Delta\sigma < \sqrt{u}N^{(1-g_f/2)}$ and $\sigma < 1/uN^{(1-g_f)}$ (random coil); (ii) $\Delta\sigma < \sqrt{\sigma/N}$ and $\sigma > 1/uN^{(1-g_f)}$ (collapsed globule); (iii) $\Delta\sigma > 1/\sqrt{u}N^{(1-g_f/2)}$ and $\Delta\sigma > u^x\sigma^y$, when $\sigma < 1/uN^{(1-g_f)}$ and $\sigma > 1/uN^{(1-g_f)}$, respectively (polyelectrolyte), where $x = 1/2(1-g_f)$ and $y = (1-g_f/2)/(1-g_f)$; (iv) $\sqrt{\sigma}/\sqrt{N} < \Delta\sigma < u^x\sigma^y$ for $\sigma > 1/uN^{(1-g_f)}$ (necklace chain, for polyampholytic homo-chains and ''hybrid chain'' when amino-acid-composed polyampholytes, like peptides, are considered). Parameter $u = l_B/L$ [29, 31, 43] compares the Bjerrum length $l_B = e^2/4\pi\varepsilon_B k_B T$ with the characteristic scale L associated with chain flexibility (typically $L \approx 2a_o$ and $\varepsilon_B \approx \varepsilon$ or ε' for each peptide, as provided by the PLLCEM; alternatively $L \approx 3.8$ Å, which is the distance between consecutive C_α in the backbone chain). When the solvent includes salt, one should expect a Coulombic screening effect for both the fluctuation-attractive electrostatic forces promoting the collapsed globule conformation and the electrostatic repulsion forces approaching the chain toward the polyelectrolyte conformational state. It should be observed that the experimental protocol used here has a solvent quite low in salt. These relationships together with the chain packing dimension and friction power coefficient may provide relevant insights concerning the microstructure of peptides (Section 3).

It is appropriate to point out here that the global structural property g_f and the scaling relationships presented above are applicable to peptides with relatively high N as a consequence of using the chain gyration radius R. Despite this important constraint, we decided to apply them also to small peptides (say $N < 9$) within the 102 peptides studied *via* the PLLCEM. The purpose was to visualize the limits of the results obtained here as discussed below.

Finally, peptide transport properties may be evaluated with numerical values Ω and a_H, as provided by the

PLLCEM at the running protocol conditions through the following expressions,

$$f = 6\pi\eta a_H/\Omega \quad (3)$$

$$s = \Omega M(1 - \nu_p/\nu_w)/\{6\pi\eta a_H N_A\} \quad (4)$$

$$D = k_B T\Omega/6\pi\eta a_H \quad (5)$$

where the effect of the shape-orientation factor, apart from the hydrodynamic radius, may also be visualized. In particular, only for near spherical particles, and to a good approximation for aspherical particles with a random flight orientation distribution function [13, 20], $D \propto a_H^{-1}$ because $\Omega \approx 1$. Furthermore, as the scaling law of the intrinsic viscosity satisfies $[\eta]_o \propto N^A$, the Mark–Houwink exponent $A \approx 3g_f - 1$ presents a quite complex relationship with physicochemical parameters included in Eq. (2), when peptide chains are considered. Thus, Ω introduces an additional effect on $[\eta]_o$ that accounts for chain packing dimension and average particle orientation (see below).

3 Results and discussion

The PLLCEM was applied to the set of 102 peptides with $2 \le N \le 42$, as proposed in Section 1, to obtain their basic properties Z, Z_T, a_H, Ω, δ, ε' and ν_p, provided by this model. Therefore, Eqs. (1)–(5) were used to evaluate the peptide global structural and transport properties. These numerical results are available in the Supporting Information (see Tables 1–3, where each peptide is coded with a number).

In general, results show that the electrical permittivity in the peptide domain is much lower than that of the solvent ($\varepsilon/\varepsilon_o \approx 80$) as expected [36]. For these peptides, it varies in the range $20 < \varepsilon'/\varepsilon_o < 46$, where ε_o is the electrical permittivity of free space (Supporting Information Table 1). Thus, ε' must be determined for each peptide AAS, avoiding in principle the use of a unique and rather arbitrary value [20] (see also [36]).

Apart from the basic properties, the meaning of which were already described in the previous studies [10, 13], an interesting aspect depicted in Supporting Information Table 1 is that peptide chain packing dimension tends to $g_p \approx 2.7$, when N increases substantially. This value was already found for some globular proteins, as reported in [20]. When $9 \le N \le 42$, for the peptides studied here $2.38 \le g_p \le 2.70$. On the contrary, this chain packing dimension falls to values smaller than 2.37, when $2 \le N \le 7$. These results suggest that smaller peptides would become more linear than those larger ones with spatial amino acid distributions similar to those of proteins. As the estimation of g_p also requires the knowledge of a_H and a_o, which are strongly coupled to charge numbers, hydration and peptide AAS, here the charge fractions $\Delta\sigma$ and σ are also considered, primarily for peptides with $N \ge 9$, through the scaling relationships provided above. Thus, it is found in general (Supporting Information Table 2) that peptides 25–27, 30, 64, 65, 67, 91 may have either globule or random coil conformations, depending mainly on the electrical permittivity used (ε or ε') and the approximate scale adopted ($L \approx 3.8$ Å or $L \approx 2a_o$), which in turn is a measure of chain flexibility. These peptides have in common $Z < \sqrt{Z_T}$, indicating that the condition for the destabilization of the globule state does not satisfy the Kantor–Kardar relationship expressed above through the equivalent equation $\Delta\sigma < \sqrt{\sigma/N}$ [44, 45]. Even in the case of peptides with lower number of amino acid residues ($N < 9$) and still with $Z < \sqrt{Z_T}$, conformational calculations indicate that small peptides behave like rather linear particles ($1.16 \le g_p \le 2.37$) with either globule or random coil conformations; depending again on the scale value L used to quantify the peptide flexibility and the environment electrical permittivity considered. Furthermore, it should be also observed that peptides 24, 62, 68, 70, 71, 73, 75, 82, 84, 85, 94, 95 have $N < 9$, but they satisfy the relationship $Z > \sqrt{Z_T}$, yielding a tendency to be in the hybrid and polyelectrolyte conformational states. In fact, these peptides have an effective charge fraction high enough to suffer destabilization, avoiding the random coil and globule conformations.

The remaining peptides studied here with $N \ge 9$ present hybrid and polyelectrolyte conformations according to the scaling relationships described above and the typical scale numbers adopted in Supporting Information Table 2. This is a clear consequence that this peptide group satisfies $Z > \sqrt{Z_T}$ and the destabilization from their globular or random coil conformations applies. Consequently, one finds effectively that peptide conformations are quite sensitive to their electrical charge state. Interesting is that peptides with hybrid conformations and relatively high N also present spatial distribution of amino acid residues with high g_p, indicating that they are not in a linear packing. These results would suggest that the tendency of peptide to form secondary structures may be quite associated with hybrid conformations, taking also into account that they approach the chain packing dimension found for proteins [20]. Furthermore, our conjecture is that for high N, peptide collapsed globule may also present secondary structure mainly as it occurs in proteins. In this sense, the transition of the hybrid/globule conformational states becomes quite important.

It must be pointed out here that the scaling relationships concerning charge number fractions $\Delta\sigma$ and σ shall be applied to each peptide without comparing their relative values with peptides of different N and AAS. In fact, the scaling relationships describing the range, where each one of the four global peptide conformational states exists, is sensitive to both N and u. For instance, Fig. 1 shows $\Delta\sigma$ as a function of σ for peptides with $N = 17$, and an average value of u to use the same plot. Furthermore, when a peptide has coordinates $\Delta\sigma$ and σ too close to the line dividing two conformational states, the possible conformations are indicated separating them through a slash in Supporting Information Table 2. Thus, one should observe here that all scaling calculations provide a simple means to extract the essential physics but do not precisely determine numerical coefficients [30].

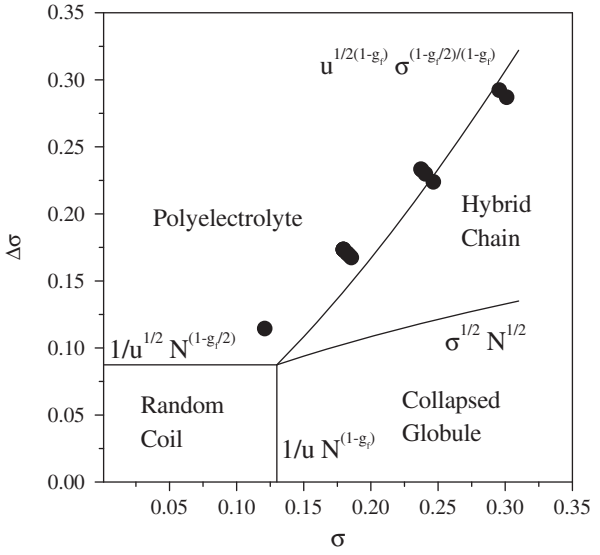

Figure 1. Effective charge number fraction $\Delta\sigma$ as a function of total charge number fraction σ, for peptides with $N = 17$ (Supporting Information Tables 1 and 2). Symbols are numerical predictions with the PLLCEM. Full lines delimit the four zones of chain conformational states. In addition, $L \approx 3.8$ Å and $\varepsilon \approx 7.07 \times 10^{-10}$ F/m. The average value $g_f \approx 0.465$ of this peptide group is used to place the data in the same plot.

In Supporting Information Table 2, values of g_f are reported. For $N \geq 9$, numerical results yield $0.38 < g_f < 0.69$, and when $Z > \sqrt{Z_T}$, some hybrid conformations are at θ-condition with $g_f \approx 1/2$ (interesting is the fact that they are not necessarily random coil polyampholytes). This range of values is in remarkable coincidence with the expected theoretical ones described in Section 2, showing the importance of knowing the peptide electrophoretic mobility *via* CZE. Furthermore, high values of g_f indicate that hybrid peptide conformations include hydrodynamic interactions in the regime of ''good solvent'' and that, under these circumstances, they behave globally as random self-avoiding chains. On the contrary, one should observe that for $g_f \leq 1/3$, the Mark–Houwink coefficient A is zero (or eventually negative for quite low N), indicating that this power law relationship does not apply in these situations and the condition of compact particles or chain globule is obtained. It is also interesting to observe that the shape-orientation factor is relevant in the evaluation of g_f (Eq. (2)). In fact, independently from the conformational state, aspherical peptides with $\Omega > 1$ tend to migrate with their major axis more parallel to the applied electrical field [13, 20], thus decreasing g_f (less free draining chain), while the opposite is true for $\Omega < 1$ because the major axis of aspherical particles migrates more perpendicular to the flow direction getting higher g_f (more free draining chain). Furthermore, as long as one may extrapolate results to low N, it is found that dipeptides 1, 3, 16 (Supporting Information Table 2) are pertinent to this analysis, where the g_f values are rather high in relation to the other dipeptides. For instance, peptide DD (in Supporting Information Tables 1 and 2) has a quite low value of packing dimension (aspherical linear chain) with an average orientation of the principal axis of around 55° ($\Omega \approx 1$) [13, 20], thus exhibiting significant free draining effects ($g_f \approx 0.74$) as expected from Eq. (2). More generally, one should find the higher values of g_f for peptides having rather linear packing dimensions (low g_p) and average orientation of the major particle axis more perpendicular to the flow direction ($\Omega < 1$) [13], what is consistent with basic hydrodynamic concepts of creeping fluid flow around particles.

The interplay between peptide packing dimension and shape-orientation factor is also relevant in relation to the Mark–Houwink relationship in viscometric analyses of polyampholytes (which must be applied for different N). In fact, this scaling law may not be applicable when these global properties are not considered specifically at each value N. More precisely, for polyampholytic chains, it is not simple to evaluate each packing dimension and shape-orientation factor *via* viscometry, when N is varied. This aspect could explain the difficulty found frequently to use effectively the Mark–Houwink relationship with some electrically charged chains in dilute solutions, apart from the well-known effect of a variable I with polyampholyte concentration [46].

It should be clear that the PLLCEM is valid for cases in which the phenomenon of ion relaxation is small and may be neglected (Debye–Hückel–Henry approximations are introduced). Thus, in this model, one expects to use values of the effective electrophoretic mobility data and protocols compatible only with the approximate ranges of the following dimensionless coordinates: $Y = 3\mu_p\eta e/(2\Omega f(\kappa a_H)\varepsilon k_B T) < 2.5$, $X = e\zeta/(k_B T) < 2.5$ and $P = \kappa a_H < 3$, with $Y \cong X$ as reported previously and also fully discussed elsewhere [13, 20]. When these constraints are not satisfied, the distortion of the counter-ion cloud around the migrating particle is found causing a reduction of the effective mobility. Ion relaxation deserved intensive research in the literature ([16, 17] and citations therein). Consequently, here we point out that around 10 peptides output data (peptides 66, 69, 72–78) obtained with the PLLCEM and reported in Supporting Information Table 1, are considered approximations to more realistic results because their coordinate X values are around the acceptable limit due to their relatively high effective charge numbers. From this table, one finds that the 102 peptides studied in this work have $0.8 < Z < 16$.

Finally, we decided to illustrate the estimation of the diffusion coefficient of the 102 peptides in Fig. 2 (Supporting Information Table 3). These values compare well with those reported by other authors [11, 12]. Here, full-line curves depicting D as a function of a_H show how the shape-orientation factor Ω varies from one peptide to another. Thus, in general, one observes that the hydrodynamic radius is not enough to quantify the diffusion

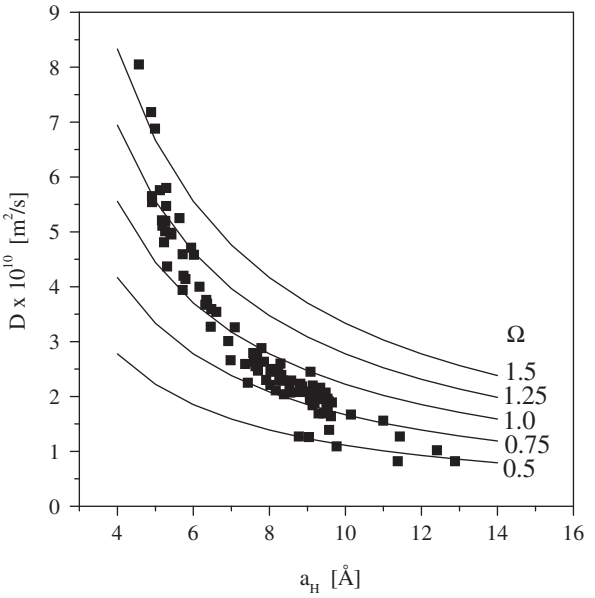

Figure 2. Average diffusion coefficient *D* as a function of peptide hydrodynamic radius a_H and shape-orientation factor Ω (Supporting Information Table 3). Symbols are numerical predictions with the PLLCEM of the 102 peptides studied here. Full lines indicate curves for constant shape-orientation factors. Line with $\Omega \approx 1$ refers to spherical particles, and to a good approximation to aspherical particles with a random flight orientation distribution function of their major axes.

coefficient of peptides, at least one can assure that the hydrodynamic particle resulting from the composition of the chain and associated water molecules has $\Omega \approx 1$, satisfying the particular conditions pointed out above. In addition, it was observed that diffusion coefficients reported *via* CZE may be weakly affected by the orientation of the particle due to the applied electrical field. Thus, diffusion coefficients obtained *via* CZE differ slightly from those values found *via* sedimentation coefficients, where a random flight orientation distribution function, in principle, may be applied [13, 20].

4 Concluding remarks

From the basic physicochemical properties of peptides obtained with the PLLCEM, it is possible to define global structural and transport properties that are closely related to their chain conformations in the peptide hydrodynamic volume. It is showed that the packing dimension, the friction power coefficient and the charge number fractions provide clues about the presence of secondary structures in peptides. In this sense, scaling relationships are helpful to indicate different chain behaviors mainly when the number of amino acid residues is relatively high. Thus, we may obtain the tendency to a given conformational state having as a reference the Kantor–Kardar line relating the effective and total charge number fractions, together with the packing dimension (linear to spatial distributions of amino acid residues) and the friction power coefficient (chain free draining intensity). Further researches should consider these physical aspects also to study proteins, for which one would expect as relevant phenomenon the transition from globule to hybrid conformations. In future researches, emphasis should be placed in the estimation of the characteristic scale associated with chain flexibility, which varies from one peptide to another, this being an intrinsic property conferred by the AAS.

The authors are grateful for financial aid received from CONICET (PIP-112-200801-01106) and UNL (CAI+D-2009-68-345).

The authors have declared no conflict of interest.

5 References

[1] Kašička, V., *Electrophoresis* 2006, *27*, 142–175.

[2] Kašička, V., *Electrophoresis* 2008, *29*, 179–206.

[3] Mittermayr, S., Olajos, M., Chovan, T., Bonn, G. K., Guttman, A., *Trends Anal. Chem.* 2008, *27*, 407–417.

[4] Kašička, V., *Electrophoresis* 2010, *31*, 122–146.

[5] Cifuentes, A., Poppe, H., *J. Chromatogr. A* 1994, *680*, 321–340.

[6] Cifuentes, A., Poppe, H., *Electrophoresis* 1995, *16*, 516–524.

[7] Adamson, N. J., Reynolds, E. C., *J. Chromatogr. B* 1997, *699*, 133–147.

[8] Jalali-Heravi, M., Shen, Y., Hassanisadi, M., Khaledi, M. G., *Electrophoresis* 2005, *26*, 1874–1885.

[9] Jalali-Heravi, M., Shen, Y., Hassanisadi, M., Khaledi, M. G., *J. Chromatogr. A* 2005, *1096*, 58–68.

[10] Piaggio, M. V., Peirotti, M. B., Deiber, J. A., *Electrophoresis* 2006, *27*, 4631–4647.

[11] Xin, Y., Mitchell, H., Cameron, H., Allison, S. A., *J. Phys. Chem. B* 2006, *110*, 1038–1045.

[12] Germann, M. W., Turner, T., Allison, S. A., *J. Phys. Chem. A* 2007, *111*, 1452–1455.

[13] Peirotti, M. B., Piaggio, M. V., Deiber, J. A., *J. Sep. Sci.* 2008, *31*, 548–554.

[14] Pei, H., Xin, Y., Allison, S. A., *J. Sep. Sci.* 2008, *31*, 555–564.

[15] Pei, H., Allison, S. A., *J. Chromatogr. A.* 2009, *1216*, 1908–1916.

[16] Allison, S. A., *Macromolecules* 1996, *29*, 7391–7401.

[17] Allison, S. A., *Biophys. Chem.* 2001, *93*, 197–213.

[18] Piaggio, M. V., Peirotti, M. B., Deiber, J. A., *Electrophoresis* 2005, *26*, 3232–3246.

[19] Piaggio, M. V., Peirotti, M. B., Deiber, J. A., *Electrophoresis* 2007, *28*, 3658–3673.

[20] Piaggio, M. V., Peirotti, M. B., Deiber, J. A., *Electrophoresis* 2009, *30*, 2328–2336.

[21] Chow, P. Y., Fasman, G. D., *Biochemistry* 1974, *13*, 211–222.

[22] Arteca, G. A., *Can. J. Chem.* 1995, *73*, 241–248.

[23] Xiong, H., Buckwalter, B. L., Shieh, H.-M., Hecht, M. H., *Proc. Natl. Acad. Sci. USA* 1995, *92*, 6349–6353.

[24] Liu, H., Yao, X., Xue, C., Zhang, R., Liu, M., Hu, Z., Fan, B., *Anal. Chim. Acta* 2005, *542*, 249–259.

[25] Zhong, L., Johnson, C., *Proc. Natl. Acad. Sci. USA* 1992, *89*, 4462–4465.

[26] Plasson, R., Vayaboury, W., Giani, O., Cottet, H., *Electrophoresis* 2007, *28*, 3617–3624.

[27] Šolínová, V., Kašička, V., Koval, D., Hlaváček, J., *Electrophoresis* 2004, *25*, 2299–2308.

[28] Flory, P. J., *Principles of Polymer Chemistry*, 9th Edn, Cornell University Press, London 1975.

[29] Dobrynin, A. V., Rubinstein, M., Joanny, J.-F., *Macromolecules* 1997, *30*, 4332–4341.

[30] Rubinstein, M., Colby, R. H., *Polymer Physics*, 1st Edn. Oxford University Press, Oxford 2004.

[31] Dobrynin, A. V., Colby, R. H., Rubinstein, M., *J. Polym. Sci. Part B Polym. Phys.* 2004, *42*, 3513–3538.

[32] Janini, G. M., Metral, C. J., Isaaq, H. J., Muschick, G. M., *J. Chromatogr. A* 1999, *848*, 417–433.

[33] Janini, G. M., Metral, C. J., Isaaq, H. J., *J. Chromatogr. A* 2001, *924*, 291–306.

[34] Antosiewicz, J., McCammnon, J. A., Gilson, M. K., *Biochemistry* 1996, *35*, 7819–7833.

[35] Allison, S. A., Carbeck, J. D., Chen, C., Burkes, F., *J. Phys. Chem. B* 2004, *108*, 4516–4524.

[36] Bashford, D., *Front. Biosci.* 2004, *9*, 1082–1099.

[37] Tanford, Ch., Physical Chemistry of Macromolecules, Wiley, USA 1961.

[38] García de la Torre, J., Huertas, M. L., Carrasco, B., *Biophys. J.* 2000, *78*, 719–730.

[39] García de la Torre, J., *Biophys. Chem.* 2001, *93*, 159–170.

[40] Russell, W. B., Saville, D. A., Schowalter, W. R., *Colloidal Dispersions*, Cambridge University Press, Cambridge, UK 1989.

[41] Larson, R. G., *Constitutive Equations for Melts and Solutions*, Butterworths, Boston, USA 1987.

[42] Yamakov, V., Milchev, A., Limbach, H. J., Dünweg, B., Everaers, R., *Phys. Rev. Lett.* 2000, *85*, 4305–4308.

[43] Higgs, P. G., Joanny, J.-F., *J. Chem. Phys.* 1991, *94*, 1543–1553.

[44] Kantor, Y., Kardar, M., *Phys. Rev. E* 1995, *51*, 1299–1312.

[45] Kantor, Y., Kardar, M., *Phys. Rev. E* 1995, *52*, 835–846.

[46] Fuoss, R. M., *J. Polym. Sci.* 1954, *12*, 185–198.

